Pergamon

Geochimica et Cosmochimica Acta, Vol. 62, No. 12, pp. 2167–2177, 1998

0016-7037/98 $19.00 + .00

PII S0016-7037(98)00132-X

Accretion and core formation on Mars: Molybdenum contents of melt inclusion glasses in three SNC meteorites

KEVIN RIGHTER,[1] RICHARD L. HERVIG,[2] and DAVID A. KRING,[3]

[1]Lunar and Planetary Laboratory, University of Arizona, Tucson, Arizona 85721, USA
[2] Center for Solid State Science, Arizona State University, Tempe, Arizona 85287, USA
[3] Lunar and Planetary Laboratory, University of Arizona, Tucson, Arizona 85721, USA

(*Received August* 20, 1997; *accepted in revised form March* 23, 1998)

Abstract—Molybdenum, cerium, barium, yttrium, and rubidium contents of glasses in melt inclusions in three SNC meteorites (LEW 88516, Governador Valadares, and Chassigny) have been measured by ion microprobe. Ratios of Mo/Ba and Mo/Ce have been used to estimate the Mo content of the primitive Martian mantle, 120 ± 60 ppb. Abundances of five moderately siderophile elements (Ni, Co, Mo, W, and P) and Re in the Martian mantle are consistent with metal-silicate equilibrium between S-bearing metallic liquid (in a core 22 wt% of the planet) and peridotite melt at 75 kb, 1620°C, and oxygen fugacity 1.4 logfO_2 units below the IW buffer. This homogeneous accretion scenario is different than many heterogeneous accretion models for the Earth, but similar to recent studies suggesting homogeneous accretion in the presence of a deep terrestrial magma ocean. *Copyright © 1998 Elsevier Science Ltd*

1. INTRODUCTION

Siderophile elements are those which partition readily into a metallic phase over silicates. As such, these elements can be sensitive indicators of metal-silicate equilibrium and core formation processes in planets and asteroids. Specifically, measured or estimated primitive mantle abundances of siderophile elements can be used to constrain conditions prevailing during core formation and accretion (e.g., Jones and Drake, 1986; Newsom, 1985). For terrestrial samples, this approach is straightforward as we have primitive samples of the mantle that have either erupted as xenoliths in volcanic rocks or occur in alpine peridotite massifs (e.g., Jagoutz et al., 1979). Estimating the abundances of the moderately siderophile elements Ni, Co, Mo, W, and P in a planetary mantle from which we have only crustal basaltic or cumulate meteorite samples (e.g., Mars, Moon, or asteroids) is a challenge, but is still possible based on what we have learned about the relation between terrestrial mantle and basalt samples (e.g., Delano, 1986). In the case of Mars, we have twelve meteorites (SNC meteorites) that can be used to determine primitive mantle abundances of Mo, W, P, and Re: seven shergottites (basaltic and lherzolitic), three nakhlites (augite-olivine cumulates), one Chassignite (olivine cumulate), and one orthopyroxenite (McSween, 1994).

The moderately siderophile elements can be divided into two groups based on their compatibility during any mantle melting or fractionation process: Mo, W, P, and Re are incompatible because their partition coefficients for most igneous phases are $\ll 1$, whereas Ni and Co are compatible because partition coefficients are >1 for many mantle phases. The concentrations of Ni and Co in the Martian mantle have been previously estimated by Wänke and Dreibus (1988), based on correlations with MgO + FeO. Concentrations of the other moderately siderophile elements (Mo, W, and P) and Re in planetary mantles can be estimated by correlations with a reference refractory lithophile element, such as La, Ce, or Yb, as long as the pair of elements exhibits nearly equal incompatibility during mantle melting and later fractionation. For the Earth, this procedure is more complicated because of the need to consider all silicate reservoirs including an extensive continental crust (e.g., Chauvel et al., 1992; Newsom et al., 1996; Sims and DePaolo, 1997). It is clear, however, that because terrestrial basalts and komatiites have the same Mo/Ba, W/Ce, P/La, and Re/Yb values as fertile mantle peridotites (e.g., Fig 1a), these ratios can be used to constrain the concentration of a given incompatible siderophile element in a primitive mantle. Similarly, shergottite basalts, or other Martian mantle melts can be used to estimate these ratios in the primitive Martian mantle.

This approach for estimating both the compatible and incompatible moderately siderophile elements was utilized by Wänke and Dreibus (1985) and Treiman et al. (1986, 1987) to show that the concentrations of Ni, Co, P, and W are consistent with a homogenous accretion scenario for early Mars. The Mo content of the Martian mantle, however, has been uncertain because only two SNC meteorite samples had been analyzed for Mo (Fig. 1b); this paucity of data for Mo (also noted recently by Lodders and Fegley, 1997) has motivated us to examine melt inclusions in three different SNC meteorites.

Many of the SNC meteorites (dunites, pyroxenites, lherzolites) contain small melt inclusions that represent trapped magma (e.g., Treiman, 1993). Although some of these inclusions have recrystallized and contain small pyroxene, amphibole, or apatite crystals, all contain large patches of glass. Since Mo and either Ba or Ce exhibit similar incompatibility (Table 1), the Mo/Ce or Mo/Ba ratios of the trapped glass should be representative of mantle Mo/Ce and Mo/Ba ratios. We have analyzed glass from inclusions in olivines from Chassigny, LEW 88516, and Governador Valadares, and these measurements, together with previous Mo and Re whole rock analyses, can be used to better define the Martian mantle Mo and Re depletions. We then used these primitive mantle abundances, predictive expressions for metal-silicate partition coefficients, and mass balance constraints to determine the conditions under which the Martian metallic core may have formed.

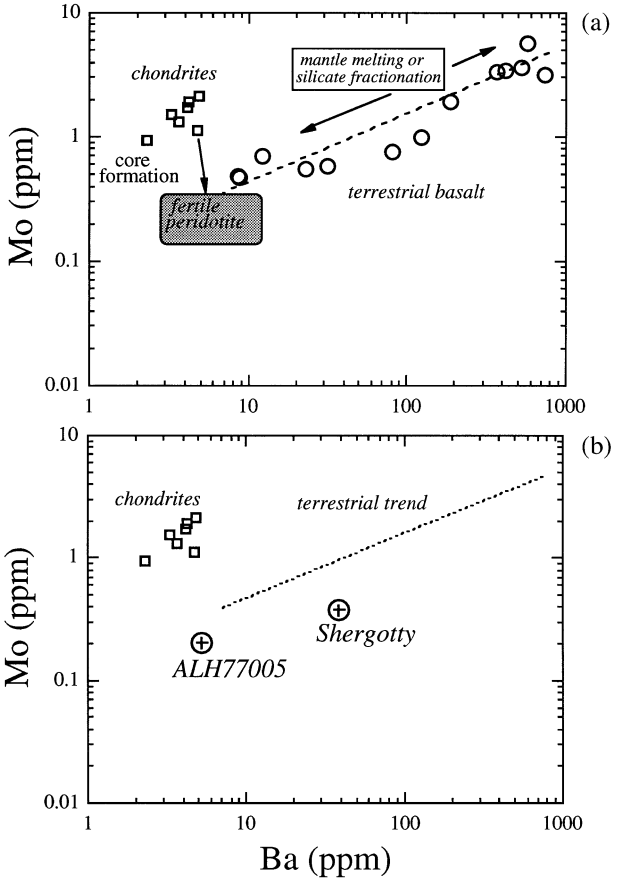

Fig. 1. (a) Molybdenum (ppm) vs. barium (ppm) data for terrestrial peridotite and basalt, compared to chondrites. Early core formation from chondritic material causes a depletion in the silicate mantle. Later melting of that mantle material produces a linear trend indicating the nearly identical incompatible behavior of Mo and Ba. Terrestrial data is from Jochum et al. (1989), Newsom and Palme (1984) and Sims et al. (1990); chondrite data is from compilation of Newsom (1995). (b) Two whole rock Mo and Ba determinations on basaltic shergottites, Shergotty, and ALHA77005 (circles with crosses); Laul et al. (1986) and Wänke et al. (1986).

2. SAMPLES

2.1. Chassigny

Chassigny is a dunite (Fo_{67}) with rare chromite and augite. Within many of the olivines are spherical and elliptical melt inclusions (Floran et al., 1978). Most of these inclusions contain crystals of orthopyroxene and augite, and a few contain kaersutitic amphibole, apatite, and biotite (Johnson et al., 1991). Some of the crystals are coarse-grained, filling one-half of the volume of the inclusion (Fig. 2a), whereas others have acicular textures (termed vitrophyric by Harvey and McSween, 1992; Fig. 2b and inclusions C1 and C2 from Table 3).

2.2. LEW 88516

LEW 88516 is a lherzolitic gabbro, comprised of mostly olivine (Fo_{64-69}) and pyroxene. The glasses in the LEW 88516 shergottite melt inclusions are unusual in that they have exsolved into two phases: a SiO_2-rich (95 wt%) phase and a more typical rhyolitic glass (Harvey et al., 1993; Gleason et al., 1997a). Since the glasses in all other melt inclusions are rhyolitic with modest alkali contents, we have focussed on this and have not analyzed the silica-rich glasses. Many of the LEW 88516 melt inclusions have similar acicular crystalline textures (Fig. 2c and 2d); crystalline phases are most commonly augite, with minor orthopyroxene, chromite, apatite, and ilmenite (see also Harvey et al., 1993).

Table 1: Summary of crystal-melt partition coefficients for Mo, Ce and Ba

Phase	D (Mo)	D (Ce)	D (Ba)	references (Mo,Ce,Ba)
olivine	0.06-0.16	0.0001	0.00001-0.00005	13,1,5
orthopyroxene	0.27	0.0001-0.002	0.004-0.01	13,5,5
augite	0.05	0.1	0.0008-0.002	1,1,6
spinel	0.2-0.5	0.006-0.02	0.05-0.30	7,8,12
plagioclase	0.39	0.044	0.14-0.6	13,1,3
apatite	-	10	<0.05	-, 11, 10
garnet	0.42	0.02	0.00001-0.00006	9,4,2

1) Jones (1995); 2) Beattie (1993a); 3) Drake and Weill (1975); 4) Shimizu and Kushiro (1975); 5) Beattie (1993b); 6) Shimizu (1974); 7) Tacker and Candela (1987); 8) Nagasawa et al. (1980); 9) Irving (1978); 10) Paster et al. (1974); 11) Watson and Green (1981); 12) Stanton (1994); 13) Dunn and Sen (1994).

2.3. Governador Valadares

The mineralogy and petrology of the Governador Valadares nakhlite have been described by Berkley et al. (1980); this clinopyroxenite contains small amounts of fayalitic (Fo_{33}) olivine. The melt inclusions within Governador Valadares olivines are of two types: some contain large single crystals of augite, minor titanomagnetite, and thin slivers of glass (Fig 2e and 2f), while others exhibit acicular crystalline textures such as described in Chassigny (Johnson et al., 1991) and LEW 88516 (Harvey and McSween, 1992). The bulk composition of all material within the inclusions was estimated by Harvey and McSween (1992); they noted the presence of thin crescents of glass at the outer edge of several inclusions, and we have analyzed two such regions for our study (Fig 2e and 2f). These types of glassy regions are ideal because they are single phase, homogeneous, and large enough to analyze with the ion microprobe without having the ions overlap with crystalline material.

3. ANALYSES

3.1. Electron Microprobe

Major and minor element contents of the melt inclusion glasses were analyzed with a CAMECA SX50 electron microprobe at the University of Arizona. Standards used for these analyses include diopside glass (Ca, Mg, Si), potassium feldspar (K, Al), apatite (P), rutile and ilmenite (Ti), fayalite (Fe) and albite (Na). Standard operating conditions were 15 kV accelerating voltage, 10 nA sample current, and a point beam. For Chassigny and Governador Valadares, in cases where volatilization was affecting alkali analyses, a rastered beam was used with lower (2 nA) sample currents. For LEW 88516 glasses, 10 nA, 10 μm rastered beam was used because volatilization was particularly problematic. In all analyses, alkalis were analyzed first for 10 s in order to minimize volatilization. Microprobe analyses were taken after the ion microprobe analyses due to the greater resolution of the microprobe beam; this allowed analysis of areas as close as possible to the ion microprobe pits. For the larger inclusions, such as 88516-C (Fig. 2d), there are compositional gradients in the glass. The compositional range from eight analyses is presented later in Table 3; for all other samples the average glass compositions are reported.

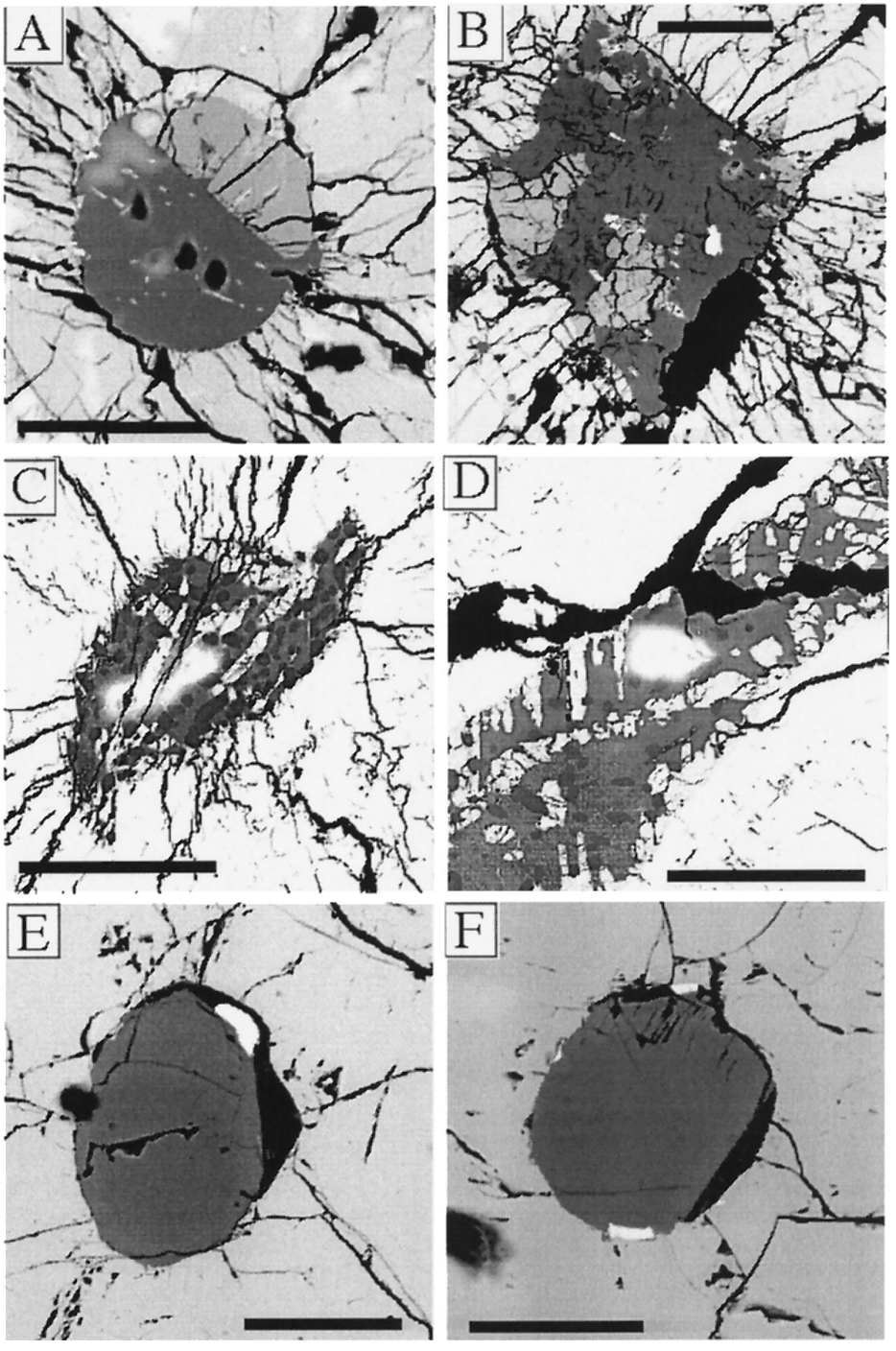

Fig. 2. Backscattered-electron (BSE) images of melt inclusions in the three SNC meteorites examined in this study. Black scale bars are 100 μm in each image. (a) and (b) are from Chassigny and are inclusions A1(1) and B3(2), respectively, in Table 3. Inclusion A1(1) is approximately one half glass and one half pyroxene. The three dark spots are the craters produced during sputtering of the glass by O-ions. The small bright crystals in the glass are apatite crystals, these were difficult to avoid, and as a result, only one of the analyses was used. Inclusion B3(2) is mostly glass (~75%) and the crystalline phases are pyroxenes. Again, the crater produced during ion sputtering is visible in the far right-hand corner of the inclusion. (c) and (d) are LEW 88516 inclusions A and C, respectively, from Table 3. The odd shape of inclusion A is a result of lengthwise shearing at some point after crystallization of pyroxenes within the inclusion; evidence for this is provided by the pyroxene-free straight edge along the shear plane. Dark rounded phases within the glass are silica-rich compositions, while the lighter grey phases in both inclusions are pyroxenes. The bright diffuse areas in both images are the craters produced during ion sputtering. (e) and (f) are from Governador Valadares and are inclusions GV1 and GV2, respectively, from Table 3. Both have large (~90%) augite crystals and minor titanomagnetite and glass (crescent-shapes at edges of inclusion).

3.2. Ion Microprobe

Measurement of Mo and Ce in the melt inclusion glasses requires a standard calibration. Since the SNC melt inclusion glasses are all silica rich and in order to minimize any possible matrix effects, we synthesized standards containing a range of Mo and Ce contents. The bulk composition is an andesite from the Mexican Volcanic Belt (#366; Righter et al., 1995), to which % levels of MoO_3 and Ce_2O_3 were added before fusing at high temperatures. The doped andesite powders were sealed within Pt capsules and heated in a Deltech resistance furnace to temperatures of 1190°C for 48 h. The liquids were quenched by removing the samples from the furnace hotspot and letting them cool to room temperature. This technique provided a rapid enough quench to preserve glass with no quench crystals. The glasses were then mounted and thin-sectioned for electron microprobe analysis (Table 2); the same standards were used for the major oxides, and Mo metal and Ce_2O_3-bearing glass were used for Mo and Ce, respectively.

The ion microprobe analyses were obtained with a primary beam of ^{16}O-ions focussed to a 10–15 μm spot at an intensity of 1.8–1.9 nA. Positive secondary ions with excess kinetic energies of 75 ± 20 eV were allowed into the mass spectrometer. This level of energy filtering effectively eliminates molecular ions containing three or more atoms from the mass spectrum, but does not completely remove dimeric ions. Each analysis consisted of a 7 min presputter period followed by collection of secondary ion intensities for ^{30}Si (10 s), ^{85}Rb (120 s), ^{89}Y (120 s), ^{98}Mo (300 s), ^{138}Ba (30 s), and ^{140}Ce (120 s), with count times indicated. The instrument was set for maximum transmission by opening the entrance slits to the mass spectrometer and using the largest (400 μm) contrast aperture. The trace element count rates were normalized to that for Si, and concentrations in the unknowns were calculated from calibration curves of $M^+/^{30}Si^+$ vs. M determined independently. Molybdenum and cerium curves were constructed with the synthetic glasses described above, together with glass standard NIST-610 (Table 2 and Fig. 3). Curves for Rb, Ba, and Y were constructed from data collected on NIST glass standards. The compositional variation in the glasses (Table 2) will affect the calculated Mo and Ce contents; the variation measured in LEW 88516 corresponds to ±3% in Mo, for example. This is minimal error relative to the counting statistics which are closer to ±15%.

Table 2: Electron and ion microprobe analyses of glasses used in Mo and Ce calibrations

Oxide	NIST 610	A	B	C	D
n	-	*13*	*14*	*15*	*15*
SiO_2	69.98	58.38	61.01	63.11	65.41
TiO_2	0.075	0.50	0.66	0.64	0.65
Al_2O_3	2.04	16.01	15.81	15.82	15.76
FeO	0.056	3.97	4.53	4.44	4.22
MgO	0.065	2.02	2.40	2.39	2.54
CaO	11.45	4.07	4.59	4.43	4.18
Na_2O	13.35	2.15	2.64	2.79	2.99
K_2O	0.059	1.97	2.10	2.26	2.39
MoO_3	396 (ppm)	4.33	1.94	1.02	0.13
Ce_2O_3	443 (ppm)	2.95	2.12	1.17	0.08
Total	97.29†	96.37	97.83	98.08	98.36
$^{98}Mo/^{30}Si+$	0.00271	0.2009	0.1233	0.0425	0.00487
duplicate	-	0.2253	0.0860	0.0421	-
$^{140}Ce/^{30}Si+$	0.0176	0.9940	0.6393	0.3525	0.04575
duplicate	-	1.2480	0.6004	0.3591	-

† total includes 0.054 MnO, 0.047 Cl-, and 0.12 P_2O_5 (data from Pearce et al., 1997)

4. RESULTS

4.1. Analytical Considerations

There are several potential problems associated with ion microprobe analysis of these elements, including the presence of apatite, dimer interferences with ^{98}Mo, and Ce anomalies (LEW 88516).

Apatite-liquid partition coefficients for Ce (and other REE) are as high as 10 (Watson and Green, 1981), and thus the presence of apatite in many of the melt inclusions presents two problems. First, overlap of the beam on an apatite crystal exposed at the surface or after some period of sputtering of the sample would result in anomalously high Ce contents. Second, if Ce is being removed from the silicate melt relative to Mo (Mo is not compatible in apatite), then the mantle Mo/Ce ratio will not be preserved. Apatites were avoided by use of reflected light and BSE images of melt inclusions before a given analytical session. If apatite was discovered near or within an ion microprobe pit after an analysis, those analyses were not used.

During sputtering of the sample, dimers are produced and if the sample contains Ti, K, Ca, and Fe there could be interference of $^{42}Ca^{56}Fe$, $^{44}Ca^{54}Fe$, $^{41}K^{57}Fe$, $^{48}Ti^{50}Ti$ dimers with ^{98}Mo. Since the glasses have very low TiO_2, CaO, and FeO contents (Table 3), these interferences will not be a problem. This was tested by examining the count rate at mass 96, where $^{40}Ca^{56}Fe$ (combining the most abundant isotopes of Ca and Fe) would be most intense. We could see no difference between the measured count rate for mass 96, and the count rate expected from the isotopic ratio of $^{96}Mo/^{98}Mo$, ~1.5:1. However, if there is overlap with an augite (~20 wt% CaO, 15 wt% FeO and 1.5–2.2 wt% TiO_2), then this interference becomes substantial. Augites were also avoided by use of reflected light and BSE images of melt inclusions before a given analytical session. If augite was discovered near or within an ion microprobe pit after an analysis, those analyses were also discarded.

Finally, Ce-anomalies (both positive and negative) are common in Antarctic meteorites (e.g., Mittlefehldt and Lindstrom, 1991; Floss and Crozaz, 1991), and LEW 88516 is no exception (Harvey et al., 1993). It may be no surprise, then, that we measured lower than chondritic Ce concentrations in the glass. For this reason, the LEW 88516 Ce data could not be used as hoped, and we only use the Ba data and the Mo/Ba ratios.

4.2. Mo/Ce and Mo/Ba Ratios

The whole rock determinations of Mo and Ce for Shergotty and ALH77005, together with the new melt inclusion glass analyses of Governador Valadares and Chassigny define a linear array. Although these data do not tightly define a line of unit slope, such a line can be fit through the data given the error associated with the analyses (Fig. 4). This trend is similar to, but just above the terrestrial Mo/Ce correlation, indicating that the depletion of Mo in the Martian mantle is not as large as in Earth's.

Cerium is most similar in incompatibility to Mo and thus is favored in geochemical comparisons (see also Sims et al., 1990). Since it is problematic in several ways in the LEW melt inclusions (as explained above) we have considered Mo-Ba

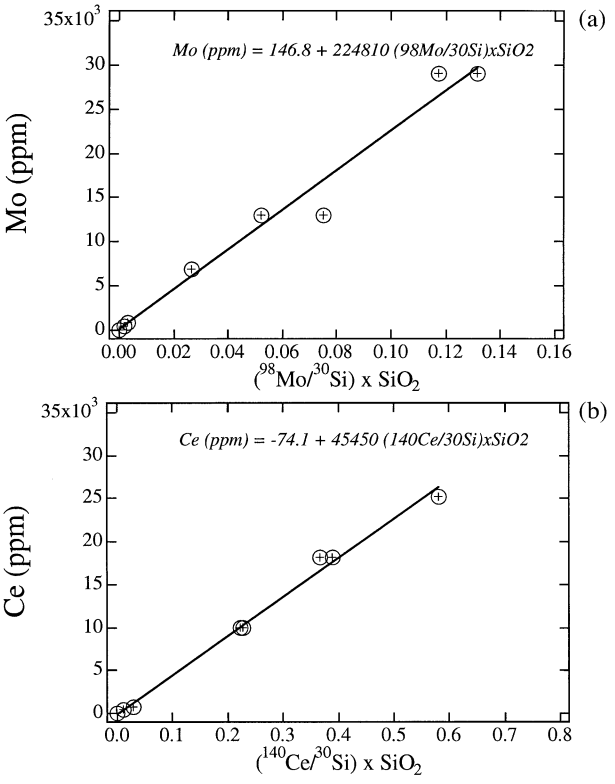

Fig. 3. Calibration curves for Mo (a) and Ce (b) secondary ion mass spectrometry (SIMS) analyses. Molybdenum, cerium, and SiO_2 are determined by electron microprobe (Table 2; see text for analytical details), and $^{98}Mo+/^{30}Si+$ and $^{140}Ce+/^{30}Si+$ are measured using SIMS techniques. Equations for each diagram are a linear fit to the data in Table 2.

trends as well; Ba exhibits incompatibility during silicate melting and has similar partition coefficients to Ce for many phases (Table 1). One advantage of Ba in this respect is that it is incompatible in apatite, in contradistinction to Ce (Table 1). Molybdenum and barium show a positive correlation in terrestrial mantle and basalt samples the same as Mo and Ce (Fig. 1a); the shallower slope of this line reflects slightly different relative partitioning relations for Mo and Ba. The large range of Ba contents in both the whole rocks (Shergotty and ALH77005) and melt inclusion glasses (Governador Valadares, Chassigny, and LEW 88516) allows the Martian Mo/Ba ratio to be well-defined. As with the Mo-Ce diagram, the melt inclusion data nicely overlap the whole rock shergottite analyses.

5. SIDEROPHILE ELEMENT CONTENT OF THE MARTIAN MANTLE

5.1. Revised Estimate of Molybdenum Content of Martian Mantle

Concentrations of Mo, W, P, and Re (1) in the Martian mantle are estimated by correlations with a reference refractory lithophile element, such as La, Ce, Ti, or Yb (r) since they exhibit nearly equal incompatibility during mantle melting. In general form the mantle concentrations can be estimated according to the relation

$$\frac{C_i^{mantle}}{C_r^{mantle}} = \frac{C_i^{basalt}}{C_r^{basalt}} \quad (1a)$$

Previous estimates of the Mo content of the SNC mantle by Treiman et al. (1987) utilized Mo/Ti ratios of Shergotty and ALH77005. Use of the Mo/Ti ratio for this study, however, is a problem due to the presence of Ti-rich phases in many of the melt inclusions. For example, melt inclusions in Governador Valadares contain titanomagnetite crystals, and those in Chassigny contain kaersutite, augite, and biotite. All of these phases concentrate Ti relative to the melt, and so the original Mo/Ti ratio of the trapped melt will be changed. For this reason, we have considered the Mo/Ce and Mo/Ba ratios to estimate the Mo content of the Martian mantle, because these two elements have similar compatibilities to Mo in a wide range of igneous minerals (see Table 1).

The Mo/Ce ratios of the SNC samples are 0.10 ± 0.05 (Fig. 4), and this translates into a mantle Mo content of 120 ± 60 ppb according to the relation

$$\frac{C_{Mo}^{mantle}}{C_{Ce}^{mantle}} = \frac{C_{Mo}^{basalt}}{C_{Ce}^{basalt}} \quad (1b)$$

where the mantle of Mars is assumed to have ~2 × CI abundances (e.g., Burghele et al., 1984) of the refractory lithophile elements (CI abundance is 603 ppb Ce; Anders and Grevesse, 1989). Consideration of the Mo/Ba ratio of 0.02 ± 0.01 (Fig. 4) in the same way results in a mantle Mo content of 95 ± 45 ppb (CI abundance is 2340 ppb Ba; Anders and Grevesse, 1989). These estimates are slightly higher than the 50 ppb estimate of Treiman et al. (1987) that was based on two shergottite analyses (and normalization to Ti), but similar to 118 ppb estimated by Wänke and Dreibus (1988). For comparison, these concentrations are slightly higher than those estimated for the terrestrial mantle (47 ppb; Sims et al., 1990; Table 4), and much higher than those for the eucrite parent body (2–6 ppb; e.g., Righter and Drake, 1997b).

5.2. Moderately Siderophile Element and Rhenium Depletions in Martian Mantle

Concentrations of a suite of moderately siderophile elements in a planetary mantle can provide information about the conditions prevailing during metal-silicate equilibrium and core formation. For Mars, the estimate obtained in the previous section for Mo can be combined with estimates for Ni, Co, W, P, and Re. The concentrations of the compatible moderately siderophile elements Ni and Co in the Martian mantle have been estimated by Wänke and Dreibus (1988), based on correlations with MgO+FeO. These concentrations are adopted here and are tabulated in Table 4.

Data for W remain sparse and include those reported by Burghele et al. (1984) for five SNC meteorites. In terrestrial and lunar basalt samples, W and La show similar incompatibility, and thus the W content of the Martian mantle may be estimated using the W/La ratio defined by the SNC meteorites. The measurements of Burghele et al. (1984), Treiman et al. (1986), and Gleason et al. (1997a) are presented in Fig. 5 and the calculated depletion in Table 4. Phosphorus and titanium were shown to be a suitable incompatible element pair, and thus

Table 3: Electron and ion microprobe analyses of melt inclusion glasses

Oxide	*LEW 88516*				*Chassigny*				*Gov. Valadares*	
	C range§	C	B	A	C1(2)	C2(2)	B3(2)	A1(1)	GV1	GV2
n		*8*	*3*	*2*	*2*	*3*	*3*	*2*	*2*	*3*
SiO_2	70.6-75.3	72.73	66.77	74.3	65.7	67.1	70.2	72.8	70.9	67.8
TiO_2	0.68-0.80	0.73	0.37	0.57	0.01	0.02	0.01	0.24	0.08	0.01
Al_2O_3	15.4-17.5	16.71	21.62	16.0	25.8	25.3	23.7	22.39	20.3	20.5
FeO	0.59-1.98	0.94	0.68	0.56	0.28	0.11	0.30	0.48	1.15	1.52
MgO	0.09-2.12	0.39	0.31	0.10	0.03	0.01	0.01	0.06	0.03	0.04
CaO	0.92-1.22	1.11	6.18	1.26	5.10	4.45	2.57	0.41	0.41	0.60
Na_2O	3.87-4.78	4.20	4.45	3.76	0.87	0.71	0.52	0.86	2.03	2.38
K_2O	3.54-4.08	3.85	0.22	3.92	0.59	1.18	2.06	2.49	4.57	5.81
P_2O_5	0.37-0.88	0.57	1.04	0.48	-	0.01	0.07	0.02	0.13	0.14
Total		101.30	102.04	100.98	98.45	98.82	99.46	99.70	99.60	98.80
Rb		114	3.1	133	12.4	9.32	23.0	45.5	63.7	354
replicate		-	-	150	14.8	-	-	-	65.0	302
Ba		41.9	11.6	22.4	702	722	681	402	541	534
replicate		-	-	17.3	832	-	-	-	535	509
Y		1.95	0.74	15.0	0.29	0.23	0.29	1.61	2.67	12.1
replicate		-	-	7.95	0.37	-	-	-	1.77	14.9
Mo		0.47	0.29	0.47	1.03	0.56	1.10	0.26	1.33	0.90
replicate		-	-	0.81	0.59	-	-	-	1.43	1.28
Ce		0.27	0.51	0.80	6.1	5.5	6.1	6.72	13.8	26.7
replicate		-	-	0.74	6.5	-	-	-	29.3	26.0

(1) and (2) denote Chassigny sections USNM 624-1 and 624-2.

§ Represents the range from 8 different analyses of glass in inclusion C; the average of these is presented in the next column, and the major element compositions reported in all other columns are averages of the indicated number of analyses.

the P content of the Martian mantle was estimated by Treiman et al. (1987) based on P/Ti ratios in SNC meteorites (Fig. 5; Table 4).

Rhenium is a highly siderophile element and present in 20–50 ppt levels in the SNC meteorites (e.g., Warren and Kallemeyn, 1996; Treiman et al., 1986; Birck and Allegre, 1994). Due to advances in analytical techniques in the past decade, there has been a large increase in the number of terrestrial and meteoritic samples analyzed for Re; as a result, it's behavior in terrestrial systems is beginning to be understood. For instance, Re is thought to be similar in behavior to Yb during mantle melting (e.g., Hauri and Hart, 1997). Rhenium is not entirely incompatible, however, as it will partition into sulfide or garnet if present (e.g., Righter and Hauri, 1997). The range of Re/Yb (ppt/ppm) in the SNC samples is 30–100 (Fig. 5); when this is considered with the 2 × CI (326 ppb) abundances of Yb, we estimate that the Martian mantle may have from 10 to 30 ppt of Re (Table 4).

6. MODELS FOR METAL-SILICATE EQUILIBRIUM BASED ON SIDEROPHILE ELEMENTS

Given the concentration estimates of Ni, Co, Mo, W, P, and Re in the Martian mantle (last section and Table 4), it is possible to ascertain under what conditions these concentrations were set during metal-silicate equilibrium and core formation. Wänke and Dreibus (1985) and Treiman et al. (1987) showed that the concentrations of Ni, Co, P, and W are consistent with a homogenous accretion scenario, based on low pressure metal-silicate partition coefficients. They were not able to reproduce the Re and Mo contents in their calculations, however. In a recent study using parameterized metal-silicate partition coefficients, Righter and Drake (1996) showed that the Ni, Co, W, P, and Mo concentrations are consistent with metal-silicate equilibrium at higher pressure and temperature conditions (60–90 kb, 1900–2000 K). Given the recent parameterization of D(Re) metal-silicate partition coefficients (Righter and Drake, 1997a), the highly siderophile element Re may be included in the present modelling. For each element, an expression of the form

$$1nD = a/T + b1nf0_2 + cP/T + d1n(1-X_S) + e(nbo/t) + f \quad (2)$$

can be derived from experimental data, and allows calculation of a metal-silicate partition coefficient as a function of pressure (P), temperature (T), oxygen fugacity (fO_2), metallic sulfur content (X_S) and silicate melt polymerization (nbo/t as defined by Mysen, 1991). Constants a through f have been derived by multiple linear regression of experimental data (see Righter et al., 1997, and Righter and Drake, 1997). These expressions can then be coupled with mass balance equations

$$\begin{aligned} C^i_{bulk} &= xC^i_{sil} + (1-x)C^i_{met} \\ C^i_{sil} &= pC^i_{LS} + (1-p)C^i_{SS} \\ C^i_{met} &= mC^i_{LM} + (1-m)C^i_{SM} \\ C^i_{sil} &= C^i_{LS}[p + (1-p)D^i_{SS/LS}] \\ C^i_{met} &= C^i_{LS}[mD^i_{LM/LS} + (1-m)D^i_{SM/LS}] \end{aligned} \quad (3)$$

where x = silicate fraction of the planet; p = fraction of the

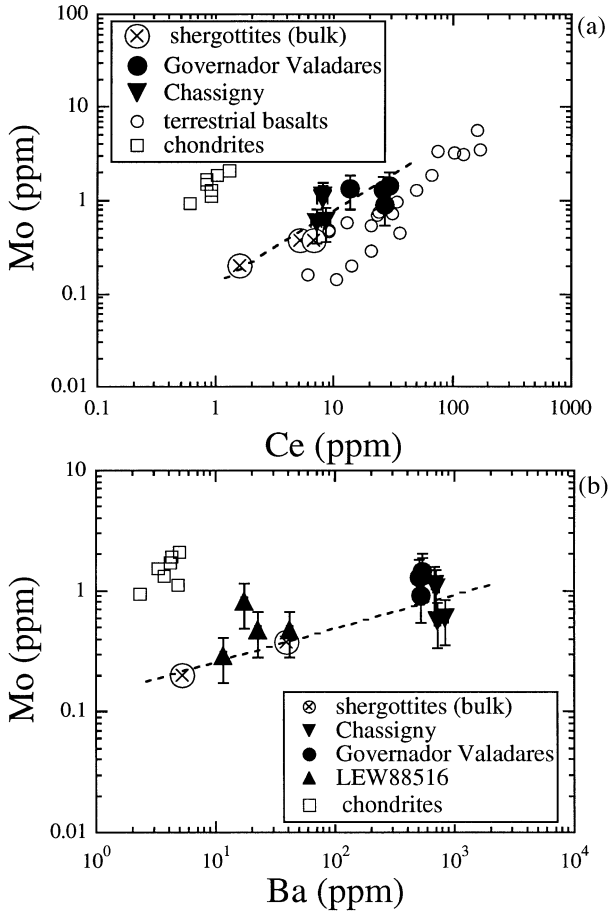

Fig. 4. Mo/Ce (a) and Mo/Ba (b) correlation diagrams for new SNC melt inclusion data for Chassigny (triangles), Governador Valadares (solid circles), and LEW 88516 (inverted triangles). Whole rock analyses of Laul et al. (1986) (Shergotty) and Wänke et al. (1986) (ALHA77005) are shown as circles with crosses. Terrestrial data is from Jochum et al (1989), Newsom and Palme (1984), and Sims et al. (1990); chondrite data is from compilation of Newsom (1995). Error bars in SIMS data represent 1σ error based on counting statistics (~15%).

Table 4: Estimated siderophile element contents of Martian mantle

	Mars (meteorites)	Mars (calculated)	Earth†
Ni (ppm)	90 (± 60)	210 (+300/-150)	1960 (± 200)
Co (ppm)	50 (± 25)	54 (+50/-30)	105 (± 10)
Mo (ppb)	120 (± 60)	32 (+100/-30)	47 (± 20)
W (ppb)	52 (+40/-25)	73 (+100/-65)	16 (± 5)
P (ppm)	600 (± 200)	625 (+600/-400)	95 (± 14)
Re (ppt)	20 (± 15)	32 (+60/-14)	280 (± 80)
H_2O§ (ppm)	10-30	-	500

† primitive upper mantle values from Jagoutz et al. (1979) (Ni and Co), Sims et al. (1990) (Mo), Newsom et al. (1996) (W) and Ringwood (1991) (P and Re).

§ from Dreibus and Wänke (1989)

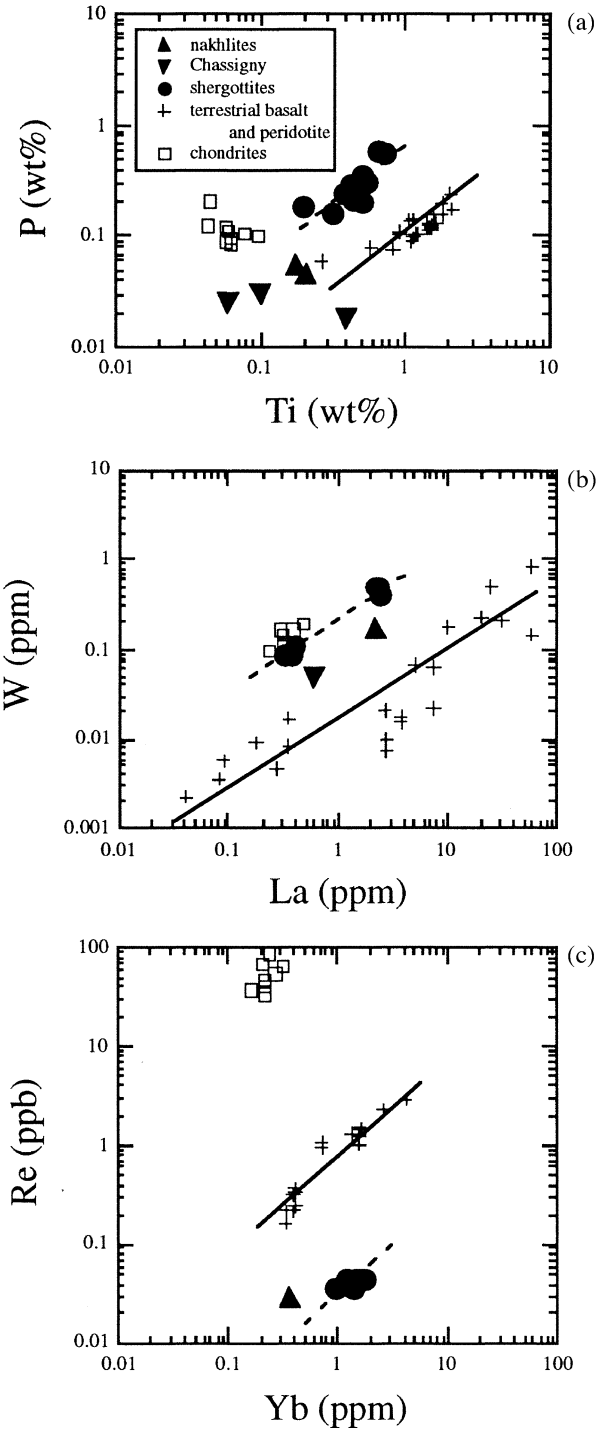

Fig. 5. P/Ti (a), W/La (b), and Re/Yb (c) data for SNC meteorites (solid dots are shergottites; upright triangles are Chassigny; inverted triangles are nakhlites), terrestrial basalt, komatiite, and peridotite (crosses; P/Ti - BVSP, 1981, Hawaii and Columbia River basalt suites; W/La - Newsom and Palme, 1984; Re/Yb - Meisel et al., 1996; Morgan, 1986; Walker et al., 1989, 1991) and chondrites (Newsom, 1995). Solid lines are drawn through terrestrial samples; dashed lines through the shergottites have the same slope as the terrestrial data. SNC P/Ti data are from the compilation of Treiman et al. (1986); W/La data are from Burghele et al. (1984), Treiman et al. (1986) and Gleason et al. (1997b); Re/Yb data are from Warren and Kallemeyn, 1996; Birck and Allègre, 1994; and Treiman et al. (1986).

silicate that is molten; and m = fraction of the metal that is molten; C^i_{sil}, C^i_{met} and C^i_{bulk} and are concentrations of siderophile elements in the silicate, metallic, and bulk portions of the planet; $D^i_{LM/LS}$ is the liquid metal/liquid silicate partition coefficient, $D^i_{SM/LS}$ is the solid metal/liquid silicate partition coefficient, and $D^i_{SS/LS}$ is the solid silicate/liquid silicate partition coefficient (e.g., Righter and Drake, 1996).

Knowing core size from moment of inertia data (~22%; e.g., Longhi et al., 1992) and linking p and m to temperature (see Righter and Drake, 1997b), this problem is reduced to six equations (one for each element) and five unknowns (T, P, fO_2, X_S, and bulk composition). The conditions under which the Martian mantle concentrations of these six elements may be fit are similar to those calculated by Righter and Drake (1996), with the exception of a smaller metallic X_S: a pressure of 75 kb, temperature of 1620°C, relative oxygen fugacity of 1.4 log fO_2 units below the IW buffer, X_S = 0.07, and a peridotite magma ocean (Fig. 6). Under these conditions, the core-forming metal would be molten (m = 1), and the mantle would be molten (p = 1) to a depth of approximately 700–800 km. As with earlier calculations (Righter and Drake, 1996) refractory lithophile elements (Ba, Ce) in the bulk composition were 2 × CI.

The sensitivity of this conclusion to changes in the intensive variables of the best fit is illustrated as follows. If all conditions are held constant except pressure which is changed to 1 bar, Mo becomes a factor of 10 lower than and W and P become a factor of 2 higher than the values based on meteorites (Table 4). Similarly changing the temperature to 1500°C causes Re to be too low, and W and Ni too high. Changes in relative redox state to IW-2 and to IW cause all elements to be lower or higher, respectively, than the meteorite-derived values (Table 4). A change in melt composition to nbo/t = 1 causes P and Re to be too low, while a change to nbo/t = 4 causes Ni, P, W, and Re to be too high. Finally, decreasing the S-content of the core metal (X_S) to zero causes the Re content to be much too low and W to be too high; for X_s = 0.3, the opposite effect occurs. It is clear from these types of illustrations, that certain elements are affected by different variables. High valence elements will be affected by small changes in redox state, more chalcophile elements are affected by small changes in S-content, and some elements are more affected by changes in T and P than others. Overall this means that there will be a limited range of conditions whereby all elements may be consistent with metal-silicate equilibrium.

6.1. Comparison with Earth

The P-T conditions for which we obtain the fit to the six siderophile elements (Fig. 6) are near liquidus conditions for the Martian mantle composition reported by Longhi et al. (1992). A pressure of 75 kb on Mars corresponds to a depths of 700–800 km: this indicates a fairly deep magma ocean (depth to the core-mantle boundary is ~2300 km). This result is similar to that obtained recently for Earth, in that the abundances of these same six siderophile elements in the primitive upper mantle can be explained by the presence of an early deep (1000 km) magma ocean floored by a metal-perovskite-magnesiowustite-bearing lower mantle (Fig. 7; see also Righter et al., 1997a). The main difference between the Martian and terrestrial results is the water content of the mantle in each case.

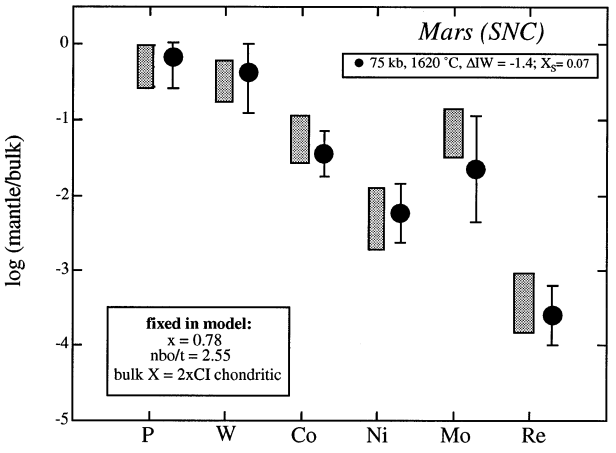

Fig. 6. Comparison of calculated and observed moderately siderophile element depletions for the Martian mantle. Shaded bars are observed depletions derived from element correlation diagrams (e.g., Figs. 4 and 5). Solid circles are calculated depletions of using partition coefficient expressions (Righter et al., 1997 for Ni, Co, Mo, W, and P; Righter and Drake, 1997a for Re) and the conditions of 75 kb, 1620°C, X_S = 0.07, relative oxygen fugacity of IW-1.4, for peridotite melt (nbo/t = 2.55). Error bars on these latter symbols represent 2σ error on the partition coefficient calculations.

The terrestrial conditions require the presence of several wt% of dissolved water in order for the mantle to be mostly molten (Fig. 7). However, the Martian case requires little to no dissolved water, because the calculated P-T conditions are near liquidus for the dry model Martian mantle composition (Longhi et al., 1992) and between the liquidus and solidus of the Allende carbonaceous chondrite (Agee et al., 1995; Fig. 7). This difference is consistent with independent estimates of water contents of each mantle: Earth has as much as 500 ppm of water in its mantle (Dreibus and Wänke, 1989), whereas estimates for Mars are relatively dry with 10–30 ppm H_2O (Dreibus and Wänke, 1989; Table 4).

Models for a terrestrial magma ocean extending to mid-mantle depths (e.g., Righter et al., 1997; Ohtani et al., 1997) provide a way of isolating the lower mantle from a vigorously convecting upper mantle. This is mainly due to the large thermal stability of perovskite (manifested by the cusp at ~25 GPa in Fig. 7) which provides a natural floor for a magma ocean. The results for Mars, while just as deep, are at much lower pressures. There are no phases that would produce an equivalent cusp for Mars at these pressures (e.g., Bertka and Fei, 1997). An olivine flotation layer at a depth of ~80 kb (Agee and Walker, 1988) may provide a temporary barrier to metal migration into a core (this would be consistent with the 15–30 Ma time constraints on core formation provided by tungsten isotope measurements of Lee and Halliday (1997), but would not cause long-term layering in the mantle in the same manner as perovskite.

The style in which planetary mantles evolve can ultimately be related to the different initial P-T conditions under which the mantle-core systems equilibrated. Positive correlations of isotopic heterogeneities (^{146}Sm-^{142}Nd: Harper et al., 1994 and ^{182}W/^{184}W: Lee and Halliday, 1997) have been documented in SNC meteorites, suggesting a coupling between metal-silicate

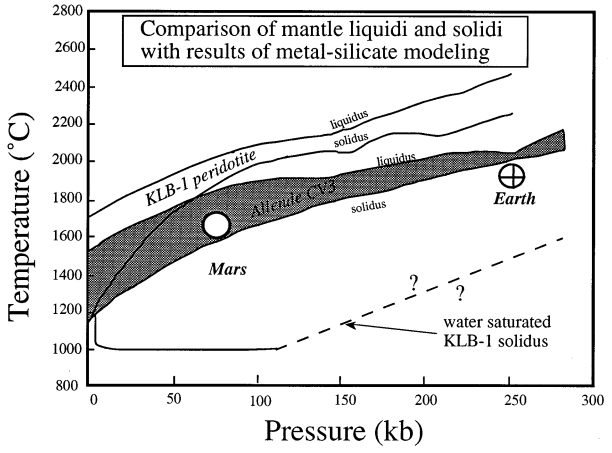

Fig. 7. P-T phase diagram for Allende (Agee et al., 1995) and KLB-1 (Zhang et al., 1994) to 30 GPa, showing the dry liquidus and solidus for each composition, together with the hydrous solidus for KLB-1 peridotite to 10 GPa determined by Kawamoto and Holloway (1997). Pressure-temperature conditions for metal-silicate equilibrium derived from siderophile element modeling for Mars (in this study) and Earth (Righter and Drake, 1997b). Note the location of the terrestrial fit below the KLB-1 and Allende solidi (at ~25 GPa), and the Martian fit between the Allende liquidus and solidus (at 6–9 GPa).

segregation and early partial melting in Mars. Geological (presence of the long-lived volcanic region surrounding Olympus Mons), geochemical (large variations in εNd; e.g., Jones, 1989; Gleason et al., 1997b) and geophysical (e.g., Harder and Christenen, 1996) observations indicate localized large-scale mantle convection on Mars. The high εNd values calculated for shergottites (>20 at 180 Ma), in particular, are in stark contrast to the depleted terrestrial mantle values of 8–12 (DePaolo, 1983; Gleason et al., 1997a). These differences between terrestrial and Martian mantle evolution highlight the importance of integrating core formation, mantle differentiation, and subsequent dynamics. Terrestrial scenarios indicate high pressure and temperature metal-silicate equilibrium fostered by an early magma ocean, followed by later (>100 Ma after formation of iron meteorite parent bodies) mantle crystallization and thermal layering, whereas Martian scenarios indicate relatively lower pressure and temperature metal-silicate equilibrium accompanied by mantle crystallization followed by later thermal history involving only whole mantle convection.

6.2. Late Veneers?

Highly siderophile elements (Re, Au, and the platinum group elements) in the terrestrial upper mantle are present in chondritic relative abundances (e.g., Morgan, 1986). Because the low pressure metal-silicate partition coefficients for these elements are very large, and different from each other, the addition of a late accretional veneer of chondritic material (~1% of the mass of the Earth) has often been proposed as a source of these elemental abundances (e.g., Chou, 1978; O'Neill, 1991). In such scenarios, the highly siderophile elements are strongly depleted in the mantle during early core formation (since the partition coefficients are high: 10^6–10^{12}); later addition of the chondritic veneer then replenishes the HSE abundances back to elevated and chondritic relative values.

Hypotheses of early siderophile element depletion followed by late veneer addition are difficult to evaluate for the Earth, because there are not samples old enough to look for evidence of the early depletions. The Martian orthopyroxenite, ALH84001, is 4.5 Ga in age and thus offers an opportunity to evaluate such a hypothesis for Mars. This sample has very low Re contents (1.6 ppt: Warren and Kallemeyn, 1996); it has been suggested by some (Warren and Kallemeyn, 1996; Brandon et al., 1997) that this is evidence for early siderophile element depletion in the Martian mantle. In light of new partitioning studies of Re in silicate systems, however, this interpretation requires revision. Given the incompatibility of Re in orthopyroxene (Righter and Hauri, 1997), the low Re contents in the 84001 orthopyroxenite are due instead to the dominance of this mineral in the rock mode. The parent melt for the orthopyroxenite had higher Re contents, and within the range of Re contents measured in other shergottites (35–100 ppt; Warren and Kallemeyn, 1996). In addition, recent osmium isotopic measurements on the shergottite ALHA77005 indicate nonchondritic initial $^{187}Os/^{188}Os$ (Brandon et al., 1997), inconsistent with the addition of a late veneer of known chondrite composition. Finally, our calculations above for Re indicate that metal-silicate equilibrium in the deep Martian mantle could instead account for the Re contents of the primitive Martian mantle. This latter hypothesis awaits further evaluation from other HSEs, as it does for the Earth.

7. CONCLUSIONS

Molydenum, cerium, barium, yttrium, and rubidium contents of glasses in melt inclusions in three SNC meteorites (LEW 88516, Governador Valadares, and Chassigny) have been measured by ion microprobe. Ratios of Mo/Ba and Mo/Ce have been used to estimate the Mo content of the primitive Martian mantle, 120 ± 60 ppb. Abundances of the moderately siderophile elements (Ni, Co, Mo, W, and P) and Re in the Martian mantle are consistent with metal-silicate equilibrium under conditions of 75 kb, 1620°C, oxygen fugacity 1.4 log$f$O$_2$ units below the IW buffer and peridotite silicate liquid. This homogeneous accretion scenario is different than many heterogeneous accretion models for the Earth, but similar to recent studies suggesting homogeneous accretion in the presence of a deep terrestrial magma ocean.

Acknowledgments—We would like to thank G. Macpherson and L. Schramm for kindly loaning Smithsonian sections 624-1 and 624-2 of Chassigny; M. M. Lindstrom for loaning section LEW 88516, 21; and R. Friedman, A. J. Brearley, and K. Keil for loaning section UNM-480 of Governador Valadares. Discussions with and comments of M. J. Drake are greatly appreciated. Journal reviews of A. H. Treiman and K. W. W. Sims helped to clarify the presentation of this work. This research is supported through NASA Grants NAGW-3348, NAG5-4084, and NAGW-3373.

REFERENCES

Agee C. B. and Walker D. (1988) Static compression and olivine flotation in ultrabasic silicate liquid. *J. Geophys. Res.* **93,** 3437–3449.

Agee C. B., Li J., Shannon M. C., and Circone S. (1995) Pressure-

temperature diagram for the Allende meteorite. *J. Geophys. Res.* **100,** 17,725–17,740.

Anders E. and Grevesse N. (1989) Abundances of the elements: Meteoritic and solar. *Geochim. Cosmochim. Acta* **53,** 197–214.

Basaltic Volcanism Study Project (1981) *Basaltic Volcanism on the Terrestrial Planets.* Pergamon Press.

Beattie P. (1993a) Uranium-thorium disequilibria and partitioning on melting of garnet peridotite. *Nature* **363,** 63–65.

Beattie P. (1993b) Trace element partitioning between silicate melts and olivines and orthopyroxenes. *Geochim. Cosmochim. Acta* **57,** 47–53.

Berkley J. L., Keil K., and Prinz M. (1980) Comparative petrology and origin of Governador Valadares and other nakhlites. *Proc. 11th Lunar Planet. Sci. Conf.*, 1089–1112.

Bertka C. M. and Fei Y. (1997) Mineralogy of the martian interior up to core-mantle boundary pressures. *J. Geophys. Res.* **102,** 5251–5264.

Birck J. L. and Allègre C. J. (1994) Contrasting Re/Os magmatic fractionation in planetary basalts. *Earth Planet. Sci. Lett.* **124,** 139–148.

Brandon A. D., Walker R. J., Morgan J. W., and Goles G. G. (1997) Rhenium-187/Osmium-187 isotopic constraints on the chemical evolution of the martian mantle. *Seventh Annual V. M. Goldschmidt Conf.; LPI Contribution No. 921, p. 35 (abstr).*

Burghele A. et al. (1984) Chemistry of shergottites and the shergotty parent body (SPB): Further evidence for the two component model of planet formation. *Lunar Planet. Sci.* **XIV,** 80–81.

Chauvel C., Hofmann A. W., and Vidal P. (1992) HIMU-EM: The French Polynesian connection. *Earth Planet. Sci. Lett.* **110,** 99–119.

Chou C. L. (1978) Fractionation of siderophile elements in the Earth's upper mantle. *Proc. 9th Lunar Planet. Sci. Conf.*, 219–230.

Delano J. W. (1986) Abundances of cobalt, nickel, and volatiles in the silicate portion of the Moon. In *Origin of the Moon* (ed. W. K. Hartmann et al.), pp. 231–248. LPI.

DePaolo D. J. (1983) The mean life of continents: estimates of continent recycling rates from neodymium and hafnium isotopic data and implications for mantle structure. *Geophys. Res. Lett.* **10,** 705–708.

Drake M. J. and Weill D. F. (1975) Partition of strontium, barium, calcium, yttrium, Eu^{2+}, Eu^{3+}, and other REE between feldspar and magmatic liquid: An experimental study. *Geochim. Cosmochim. Acta* **39,** 689–712.

Dreibus G. and Wänke H. (1989) Supply and loss of volatile constituents during the accretion of terrestrial planets. In *Origin and Evolution of Planetary and Satellite Atmospheres* (ed. S. K. Atreya et al.), 268–289, Univ. Arizona Press.

Dunn T. and Sen G. (1994) Mineral/matrix partition coefficients for orthopyroxene, plagioclase, and olivine in basaltic to andesitic systems: A combined analytical and experimental study. *Geochim. Cosmochim. Acta* **58,** 717–733.

Floran R. J., Prinz M., Hlava P. F., Keil K., Nehru C. E., and Hinthorne J. R. (1978) The Chassigny meteorite: A cumulate dunite with hydrous amphibole-bearing melt inclusions. *Geochim. Cosmochim. Acta* **42,** 1213–1229.

Floss C. and Crozaz G. (1991) Cerium anomalies in the LEW85300 eucrite: Evidence for REE mobilization during Antarctic weathering. *Earth Planet. Sci. Lett.* **107,** 13–24.

Gleason J. D., Kring D. A., Hill D. H., and Boynton W. V. (1997a) Petrography and bulk chemistry of martian lherzolite LEW 88516. *Geochim. Cosmochim. Acta* **61,** 4007–4014.

Gleason J. D., Kring D. A., and Boynton W. V. (1997b) Divergent mantle evolution on Earth and Mars and the origin of depleted planetary mantles. *Seventh Annual Goldschmidt Conf.; LPI Contrib.* **921,** 81–82 (abstr.).

Harder H. and Christensen U. R. (1996) A one-plume model of martian mantle convection. *Nature* **380,** 507–509.

Harper C. L., Nyquist L. E., Bansal B., Wiesmann H., and Shih C.-Y. (1995) Rapid accretion and early differentiation of Mars indicated by ^{142}Nd-^{144}Nd in SNC meteorites. *Science* **267,** 213–217.

Harvey R. P., Wadhwa M., McSween H. Y., and Crozaz G. (1993) Petrography, mineral chemistry, and petrogenesis of Antarctic Shergottite LEW 88516. *Geochim. Cosmochim. Acta* **57,** 4769–4784.

Harvey R. P. and McSween H. Y. (1992) The parent magma of the nakhlite meteorites: Clues from melt inclusions. *Earth Planet. Sci. Lett.* **111,** 467–482.

Hauri E. H. and Hart S. R. (1997) Rhenium abundances and systematics in oceanic basalts. *Chem. Geol.* **139,** 185–205.

Irving A. J. (1978) A review of experimental studies of crystal/liquid trace element partitioning. *Geochim. Cosmochim. Acta* **42,** 743–770.

Jagoutz E. et al. (1979) The abundances of major, minor, and trace elements in the earth's mantle as derived from primitive ultramafic nodules. *Proc. 10th Lunar Planet. Sci. Conf.*, 2031–2050.

Jochum K. P., McDonough W. F., Palme H., and Spettel B. (1989) Compositional constraints on the continental lithospheric mantle from trace elements in spinel peridotite xenoliths. *Nature* **340,** 548–550.

Johnson M. C., Rutherford M. J., and Hess P. C. (1991) Chassigny petrogenesis: Melt inclusions, intensive parameters, and water contents of martian (?) magmas. *Geochim. Cosmochim. Acta* **55,** 349–366.

Jones J. H. (1995) Experimental race element partitioning. In *Rock Physics and Phase Relations A Handbook of Physical Constants* (ed. T. J. Ahrens); *AGU Ref. Shelf* **3,** 73–104. AGU

Jones J. H. (1989) Isotopic relations among the shergottites, the nakhlites, and Chassigny. *Proc. Lunar Sci. Conf.* **19,** 465–474.

Jones J. H. and Drake M. J. (1986) Geochemical constraints on core formation in the Earth. *Nature* **322,** 221–228.

Kawamoto T. and Holloway J. R. (1997) Melting temperature and partial melt chemistry of H_2O-saturated mantle peridotite to 11 GPa. *Science* **276,** 240–243.

Laul J. C. et al. (1986) Chemical systematics of the Shergotty meteorite and the composition of its parent body (Mars). *Geochim. Cosmochim. Acta* **50,** 909–926.

Lee D.-C. and Halliday A. N. (1997) Core formation on Mars and differentiated. *Nature* **388,** 854–857.

Lodders K. L. and Fegley B. (1997) An oxygen isotope model for the composition of Mars. *Icarus* **126,** 373–394.

Longhi J., Knittle E., Holloway J. R., and Wänke H. (1992) The bulk composition, mineralogy and internal structure of Mars. In *Mars* (ed. H. H. Kieffer et al.), pp. 184–208. Univ. Arizona Press.

McSween H. Y. (1994) What we have learned about Mars from SNC meteorites. *Meteoritics* **29,** 757–779.

Meisel T., Walker R. J., and Morgan J. W. (1996) The osmium isotopic composition of the Earth's primitive upper mantle. *Nature* **383,** 517–519.

Mittlefehldt D. W. and Lindstrom M. M. (1991) Generation of abnormal trace element abundances in Antarctic eucrites by weathering processes. *Geochim. Cosmochim. Acta* **55,** 77–88.

Morgan J. W. (1986) Ultramafic xenoliths: Clues to Earth's late accretionary history. *J. Geophys. Res.* **91,** 12375–12387.

Mysen B. O. (1991) Relations between structure, redox equilibria of iron and properties of magmatic liquids. In *Physical Chemistry of Magmas* (ed. L. L. Perchuk and I. Kushiro), pp. 41–98. Springer-Verlag.

Nagasawa H., Schreiber H. D., and Morris R. V. (1980) Experimental mineral/liquid partition coefficients of the rare earth elements (REE), scandium and strontium for perovskite, spinel, and melilite. *Earth Planet. Sci. Lett.* **46,** 431–437.

Newsom H. E. (1985) Molybdenum in eucrites: Evidence for a metal core in the eucrite parent body. *J. Geophys. Res.* **90** (suppl.), C613–C617.

Newsom H. E. (1995) Composition of the solar system, planets, meteorites, and major terrestrial reservoirs. In *Global Earth Physics: A Handbook of Physical Constants* (ed. T. J. Ahrens); *AGU Ref. Shelf* **1,** 159–189. AGU.

Newsom H. and Palme H. (1984) The depletion of siderophile elements in the Earth's mantle: New evidence from molybdenum and tungsten. *Earth Planet. Sci. Lett.* **69,** 354–364.

Newsom H. E., Sims K. W. W., Noll P. D. Jr., Jaeger W. L., Maehr S. A., and Beserra T. B. (1996) The depletion of tungsten in the bulk silicate earth: Constraints on core formation. *Geochim. Cosmochim. Acta* **60,** 1155–1169.

O'Neill H. St.C. (1991) The origin of the Moon and the early history of the Earth - A chemical model. Part 2: The Earth. *Geochim. Cosmochim. Acta* **55,** 1159–1174.

Ohtani E., Yurimoto H., and Seto S. (1997) Element partitioning

between metallic liquid, silicate liquid, and lower-mantle minerals: Implications for core formation of the Earth. *Phys. Earth Planet. Intl.* **100,** 97–114.

Paster T. P., Schauwecker D. S., and Haskin L. A. (1974) The behavior of some trace elements during solidification of the Skaergaard layered series. *Geochim. Cosmochim. Acta* **38,** 1549–1577.

Pearce N. J. G. et al. (1997) A compilation of new and published major and trace element data for NIST SRM 610 and NIST SRM 612 glass reference materials. *Geostand. Newsl.* **21,** 115–144.

Righter K. and Drake M. J. (1996) Core formation in Earth's Moon, Mars, and Vesta. *Icarus* **124,** 513–529.

Righter K. and Drake M. J. (1997a) Metal-silicate equilibrium in a homogeneously accreting Earth: New results for rhenium. *Earth Planet. Sci. Lett.* **146,** 541–553.

Righter K. and Drake M. J. (1997b) A magma ocean on Vesta: Core formation and petrogenesis of eucrites and diogenites. *Met. Planet. Sci.* **32,** 929–944.

Righter K. and Hauri E. H. (1997) Rhenium is compatible in garnet during mantle melting and magma genesis. *Seventh Annual V.M. Goldschmidt Conf., LPI Contrib. 921,* p. 175 (abstr.).

Righter K., Drake M. J., and Yaxley G. (1997) Prediction of siderophile element metal-silicate partition coefficients to 120 kb and 2800°C: The effect of pressure, temperature, fO_2, and melt composition. *Phys. Earth Planet. Intl.* **100,** 115–134

Righter K., Carmichael I. S. E., Becker T. A., and Renne R. P. (1995) Pliocene to Quaternary volcanism and tectonism at the intersection of the Mexican Volcanic Belt and the Gulf of California. *Geol. Soc. Amer. Bull.* **107,** 612–626.

Ringwood A. E. (1991) Phase transformations and their bearing on the constitution and dynamics of the mantle. *Geochim. Cosmochim. Acta* **55,** 2083–2110.

Shimizu N. (1974) An experimental study of the partitioning of potassium, rubidium, cesium, strontium, and barium between clinopyroxene and liquid at high pressures. *Geochim. Cosmochim. Acta* **38,** 1789–1798.

Shimizu N. and Kushiro I. (1975) The partitioning of rare earth elements between garnet and liquid at high pressures: Preliminary experiments. *Geophys. Res. Lett.* **2,** 413–416.

Sims K. W. W. and DePaolo D. J. (1997) Inferences about mantle magma sources from incompatible element concentration ratios in oceanic basalts. *Geochim. Cosmochim. Acta* **61,** 765–784.

Sims K. W. W., Newsom H. E., and Gladney E. S. (1990) Chemical fractionation during formation of the Earth's core and continental crust: Clues from arsenic, antimony, tungsten, and molybdenum. In *The Origin of the Earth* (ed. H. Newsom and J. H. Jones), pp. 291–317. Oxford Press.

Stanton R. L. (1994) *Ore Elements in Arc Lavas.* Oxford Univ. Press.

Tacker R.C . and Candela P. A. (1987) Partitioning of Molybdenum between magnetite and melt: A preliminary experimental study of partitioning of ore metals between silicic magmas and crystalline phases. *Econ. Geol.* **82,** 1827–1838.

Treiman A. H., Drake M. J., Janssens M.-J., Wolf R., and Ebihara M. (1986) Core formation in the Earth and Shergottite Parent Body (SPB): Chemical evidence from basalts. *Geochim. Cosmochim. Acta* **50,** 1071–1091.

Treiman A. H., Jones J. H., and Drake M. J. (1987) Core formation in the shergottite parent body and comparison with the Earth. *J. Geophys. Res.* **92,** E627–E632.

Treiman A. H. (1993) The parent magma of the Nakhla (SNC) meteorite, inferred from magmatic inclusions. *Geochim. Cosmochim. Acta* **57,** 4753–4767.

Walker R. J., Shirey S. B., and Stecher O. (1988) Comparative Re-Os, Sm-Nd and Rb-Sr isotope and trace element systematics for Archean komatiite flows from Munro Township, Abitibi Belt, Ontario. *Earth Planet. Sci. Lett.* 87, 1–12.

Walker R. J., Echeverria L. M., Shirey S. B., and Horan M. F. (1991) Re-Os isotopic constraints on the origin of volcanic rocks, Gorgona Island, Colombia: Osmium isotopic evidence for ancient heterogeneities in the mantle. *Contrib. Mineral. Petrol.* **107,** 15–162.

Wänke H. and Dreibus G. (1985) The degree of oxidation and the abundance of volatile elements on Mars. *Lunar Planet. Sci.* **XVI,** Supp. A, 28–29.

Wänke H. and Dreibus G. (1988) Chemical composition and accretion history of terrestrial planets. *Phil. Trans. Royal Soc. London* **A325,** 545–557.

Wänke H., Dreibus G., Jagoutz E., Palme H., Spettel B., and Weckwerth G. (1986) ALHA77005 and on the chemistry of the shergottite parent body (Mars). *Lunar Planet. Sci.* **XVII,** 919–920.

Warren P. H. and Kallemeyn G. W. (1996) Siderophile trace elements in ALH84001, other SNC meteorites and eucrites: Evidence for heterogeneity, possibly time-linked, in the mantle of Mars. *Meteor. Planet. Sci.* **31,** 97–105.

Watson E. B. and Green T. H. (1981) Apatite/liquid partition coefficients for the rare earth elements and strontium. *Earth Planet. Sci. Lett.* **56,** 405–421.

Zhang J. and Herzberg C. (1994) Melting experiments on anhydrous peridotite KLB-1 from 5.0 to 22.5 GPa. *J. Geophys. Res.* **99,** 17729–17742.